Arbidol and Other Low-Molecular-Weight Drugs That Inhibit Lassa and Ebola Viruses

C. E. Hulseberg,[a]* L. Fénéant,[b] K. M. Szymańska-de Wijs,[b]* N. P. Kessler,[b] E. A. Nelson,[b] C. J. Shoemaker,[c]* C. S. Schmaljohn,[c] S. J. Polyak,[d,e] J. M. White[a,b]

[a]Department of Microbiology, University of Virginia, Charlottesville, Virginia, USA
[b]Department of Cell Biology, University of Virginia, Charlottesville, Virginia, USA
[c]Virology Division, U.S. Army Medical Research Institute of Infectious Diseases, Fort Detrick, Maryland, USA
[d]Department of Laboratory Medicine, University of Washington, Seattle, Washington, USA
[e]Department of Global Health, University of Washington, Seattle, Washington, USA

ABSTRACT Antiviral therapies that impede virus entry are attractive because they act on the first phase of the infectious cycle. Drugs that target pathways common to multiple viruses are particularly desirable when laboratory-based viral identification may be challenging, e.g., in an outbreak setting. We are interested in identifying drugs that block both Ebola virus (EBOV) and Lassa virus (LASV), two unrelated but highly pathogenic hemorrhagic fever viruses that have caused outbreaks in similar regions in Africa and share features of virus entry: use of cell surface attachment factors, macropinocytosis, endosomal receptors, and low pH to trigger fusion in late endosomes. Toward this goal, we directly compared the potency of eight drugs known to block EBOV entry with their potency as inhibitors of LASV entry. Five drugs (amodiaquine, apilimod, arbidol, niclosamide, and zoniporide) showed roughly equivalent degrees of inhibition of LASV and EBOV glycoprotein (GP)-bearing pseudoviruses; three (clomiphene, sertraline, and toremifene) were more potent against EBOV. We then focused on arbidol, which is licensed abroad as an anti-influenza drug and exhibits activity against a diverse array of clinically relevant viruses. We found that arbidol inhibits infection by authentic LASV, inhibits LASV GP-mediated cell-cell fusion and virus-cell fusion, and, reminiscent of its activity on influenza virus hemagglutinin, stabilizes LASV GP to low-pH exposure. Our findings suggest that arbidol inhibits LASV fusion, which may partly involve blocking conformational changes in LASV GP. We discuss our findings in terms of the potential to develop a drug cocktail that could inhibit both LASV and EBOV.

IMPORTANCE Lassa and Ebola viruses continue to cause severe outbreaks in humans, yet there are only limited therapeutic options to treat the deadly hemorrhagic fever diseases they cause. Because of overlapping geographic occurrences and similarities in mode of entry into cells, we seek a practical drug or drug cocktail that could be used to treat infections by both viruses. Toward this goal, we directly compared eight drugs, approved or in clinical testing, for the ability to block entry mediated by the glycoproteins of both viruses. We identified five drugs with approximately equal potencies against both. Among these, we investigated the modes of action of arbidol, a drug licensed abroad to treat influenza infections. We found, as shown for influenza virus, that arbidol blocks fusion mediated by the Lassa virus glycoprotein. Our findings encourage the development of a combination of approved drugs to treat both Lassa and Ebola virus diseases.

Address correspondence to J. M. White, jw7g@virginia.edu.

* Present address: C. E. Hulseberg, Center for Genome Sciences, U.S. Army Medical Research Institute of Infectious Diseases, Fort Detrick, Maryland, USA; K. M. Szymańska-de Wijs, Institute of Virology, Hannover Medical School, Hannover, Germany; C. J. Shoemaker, Diagnostic Systems Division, USAMRIID, Fort Detrick, Maryland, USA.

Lassa virus (LASV) is an enveloped ambisense RNA virus belonging to the *Arenaviridae*. As the most clinically significant member of this large family, LASV is a major pathogen in West Africa, where it infects an estimated 300,000 people each year. LASV has also been responsible for a number of imported cases of Lassa hemorrhagic fever (LHF) in Europe and North America in recent years (1). The 2018 outbreak of LHF in Nigeria was particularly severe, with over 430 confirmed positive cases and a case fatality rate of ~25% (2). Classic symptoms of acute LHF include malaise, headache, fever, vomiting, respiratory distress, facial edema, and hemorrhaging of mucosal surfaces (3). Even in fatal cases, however, patients may not present with redolent hemorrhagic fever symptoms, complicating diagnosis (4).

The only antiviral treatment option for LHF is the guanosine analogue ribavirin. There are a substantial number of contraindications and adverse effects associated with ribavirin, and its efficacy in clinical trial settings remains controversial and underevaluated. Furthermore, while ribavirin is effective against other hemorrhagic fever arenaviruses, it has limited efficacy against filoviruses. Thus, current guidelines recommend ribavirin only after high-risk exposures to LASV (5). Given the partial geographic overlap between Ebola virus (EBOV) and LASV in West Africa and similar clinical presentation in early infection stages, it would be advantageous to have a common therapeutic effective against both viruses (6, 7).

Promising new compounds against LASV have been identified (6, 8–17), but the limited geographical endemicity of LASV, its inefficient person-to-person transmission, and low reinfection rates make the prospect of collecting adequate clinical trial data on new drugs challenging. Thus, a practical approach to more expeditiously grow the arsenal of drugs against these highly pathogenic viruses is to screen approved drugs for antiviral activity. When this strategy was employed, many FDA-approved compounds with repurposing potential were identified that showed inhibitory effects against EBOV (18–24). Many of these are thought to act upon the entry stages of EBOV infection. A similar recent screen revealed FDA-approved drugs with potential activity against LASV (8).

Viral entry inhibitors are valuable as therapeutics, since blocking infection early in the life cycle will reduce cellular and tissue damage associated with the replication of incoming viruses and the production of viral progeny. LASV employs several key features in common with EBOV for its entry: (i) it is internalized into the endocytic pathway by a macropinocytotic-like process after initial contact with surface receptors/attachment factors, (ii) low pH is needed to trigger fusion, and (iii) an endosomal, cholesterol binding receptor promotes endosomal escape (Lamp1 for LASV and NPC1 for EBOV) (12, 25–32). Hence, for this study, we selected eight low-molecular-weight drugs shown to inhibit EBOV entry and directly compared their inhibitory activities against LASV and EBOV. Five of these drugs have FDA approval (amodiaquine, clomiphene, niclosamide, sertraline, and toremifene), one is licensed abroad (arbidol), and two have been evaluated in clinical trials (apilimod and zoniporide).

The compound we investigated in most detail was the anti-influenza drug arbidol (umifenovir), which was developed and is currently used as an antiviral. Arbidol has been reported to have inhibitory effects on a diverse array of viruses, including DNA and RNA viruses as well as capsid- and membrane-enclosed viruses (33–36). Studies aimed at determining the mechanism of action of arbidol implicate a number of possible antiviral effects, including several steps of entry as well as later phases of the infectious cycle (36). The principal inhibitory effect of arbidol on influenza virus, for which it has been a licensed treatment in China and Russia for many years, appears to be during a late stage of entry, when influenza virus fuses with an endosomal membrane. While arbidol can bind directly to influenza hemagglutinin (HA) and inhibit its ability to transition to an activated conformation (37–39), it is not yet clear whether this is its sole or primary mechanism of anti-influenza activity or if arbidol also impairs fusion by intercalation into the viral or target membrane, thereby rendering the membrane less yielding for fusion (35).
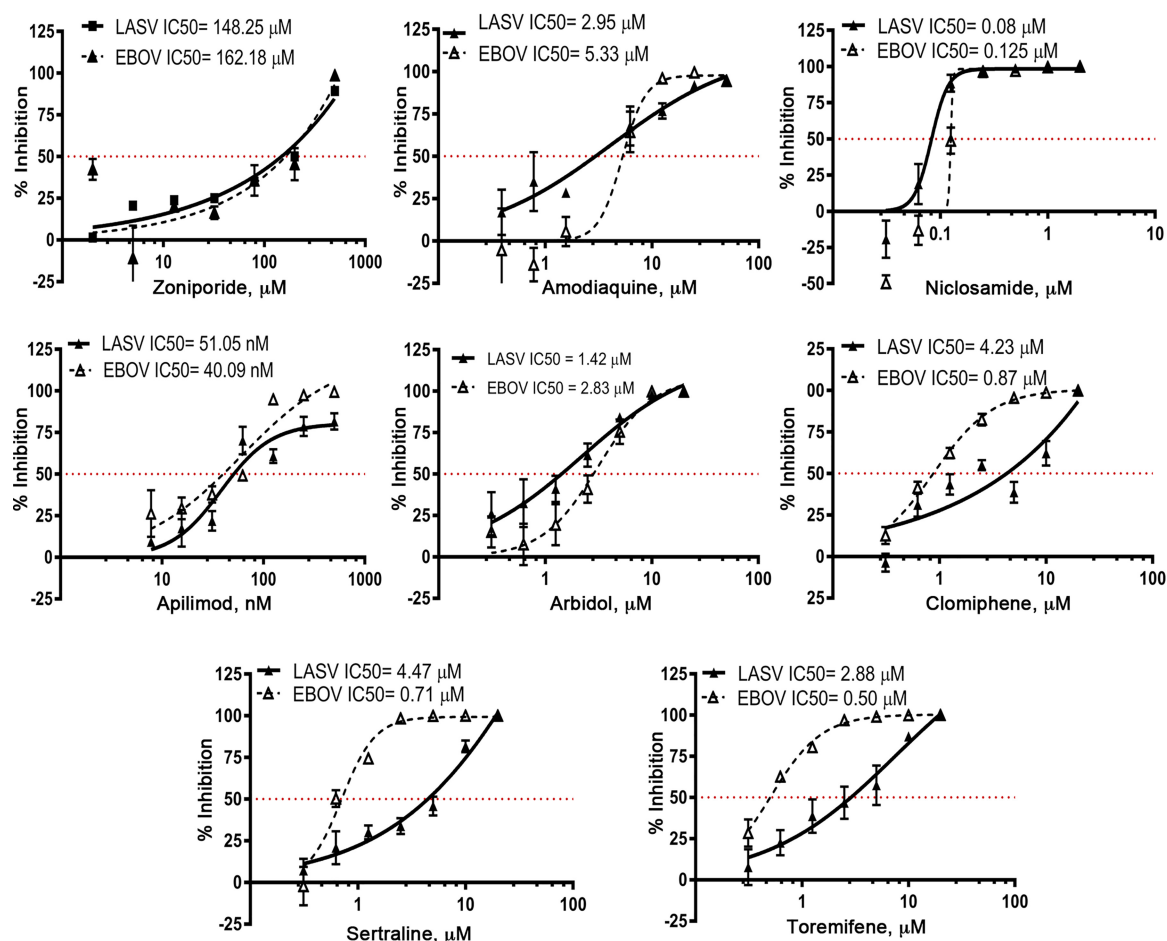
FIG 1 Representative dose response curves for eight low-molecular-weight drugs against LASV GP- and EBOV GP-mediated MLV pseudovirus infection. BSC-1 cells were pretreated with the indicated dose of the indicated drug for 1 h and then infected with MLV pseudoviruses encoding luciferase. Luciferase signals were measured 24 h later and normalized to the maximal signal from a triplicate set of mock-treated cells. Data points indicate the average percent inhibition from triplicate wells. Error bars represent the SDs. The red horizontal dashed line indicates 50% inhibition. Each dose-response comparison was conducted 3 to 5 times, with similar results.

RESULTS

Comparison of the potency of small-molecule inhibitors against LASV GP- and EBOV GP-mediated entry. Enveloped viruses that are endocytosed rely on their glycoproteins (GPs) to mediate the entire entry process, from attachment to the cell surface to fusion within endosomal membranes. In this study, we directly compared the effects of eight drugs that block EBOV entry for their effects on LASV GP-mediated entry. To do this, we used murine leukemia viruses (MLV) carrying a luciferase reporter and pseudotyped with either LASV or EBOV GP. Drug dosing ranges were determined by establishing the concentration of each drug needed to elicit a near-total inhibition of infection. The remaining doses in each set were 2-fold serial dilutions. A mock (vehicle-only) treatment was included as an anchor point in each series to assess the extent of inhibition in treated cells.

Representative direct comparative dose-response curves for LASV and EBOV for each of the eight drugs are presented in Fig. 1. Each drug was tested in parallel against LASV GP- and EBOV GP-MLV pseudoviruses in three to five independent experiments. Table 1 reports the average ratio of the 50% inhibitory concentration (IC_{50}) value against LASV GP divided by that for EBOV GP, analyzed in parallel, for each of the eight drugs tested. These ratios indicated that the IC_{50} values against LASV GP-MLV pseudoviruses for five drugs (zoniporide, amodiaquine, niclosamide, apilimod, and arbidol) were either approximately the same as or lower than the corresponding values for

TABLE 1 Comparative ability of drugs to block infections by LASV and EBOV GP-MLV pseudoviruses[a]

Drug	Step blocked	n	Avg ratio of IC_{50} for LASV to IC_{50} for EBOV, mean ± SEM
Zoniporide	Internalization	3	0.72 ± 0.14
Amodiaquine	Acidification	4	0.41 ± 0.14
Niclosamide	Acidification	5	0.54 ± 0.13
Apilimod	Traffic	3	1.50 ± 0.16
Arbidol	Fusion	3	0.59 ± 0.12
Clomiphene	Fusion	4	4.72 ± 2.41
Sertraline	Fusion	3	4.99 ± 2.37
Toremifene	Fusion	3	6.71 ± 3.09

[a]In each experiment ($n = 3$ to 5 as indicated), cells were pretreated with 8 doses of the indicated drugs and their IC_{50}s for blocking infections by LASV and EBOV GP MLV pseudoviruses were determined in triplicate samples as described in Materials and Methods. For each experiment, the following ratio was then calculated: the IC_{50} for blocking LASV GP pseudovirus infection divided by the IC_{50} for blocking EBOV GP pseudovirus infection. Values in column 4 are the averages of those ratios ± SEMs. The average IC_{50} and maximal percent inhibition values across all experiments for LASV were as follows: zoniporide, 88 μM and 87%; amodiaquine, 1.9 μM and 82%; niclosamide, 0.12 μM and 100%; apilimod, 0.04 μM and 80%; arbidol, 1.7 μM and 95%; clomiphene, 5.7 μM and 100%; sertraline, 2.6 μM and 90%; and toremifene, 2.9 μM and 96%. The average IC_{50} and maximal percent inhibition values across all experiments for EBOV were as follows: zoniporide, 115 μM and 98%; amodiaquine, 6.6 μM and 97%; niclosamide, 0.24 μM and 100%; apilimod, 0.03 μM and 100%; arbidol, 2.8 μM and 100%; clomiphene, 1.8 μM and 100%; sertraline, 0.7 μM and 100%; and toremifene, 0.5 μM and 100%. Ratios very similar to those presented in column 4 were obtained for the ratios of the average IC_{50} values across all experiments.

EBOV GP-MLV pseudoviruses, indicating similar or enhanced potency against LASV GP-mediated infection. For three drugs, clomiphene, sertraline, and toremifene, the IC_{50} values for LASV were ~3- to 6-fold greater than those for EBOV, indicating that these drugs are more potent against EBOV. It is noteworthy that these three drugs are cationic amphiphilic drugs (CADs), which may be especially active against EBOV (19, 20, 23, 40).

For the remainder of the study we focused on arbidol, for reasons outlined in the introduction. Pécheur and colleagues reported an EC_{50} of 5.8 μM in Vero cells for arbidol against the New World arenavirus Tacaribe virus (34); to the best of our knowledge, this is the only published evaluation of the efficacy of arbidol against an arenavirus. Using MLV pseudoviruses, we found that in addition to inhibiting entry mediated by LASV GP (Fig. 1), arbidol inhibited entry mediated by the GPs of two other arenaviruses, those of lymphocytic choriomeningitis virus (LCMV) and Junin virus (Fig. 2A). We also found, using MLV pseudoviruses, that arbidol is somewhat more potent against LASV GP-mediated infection than against infection mediated by influenza virus HA from the WSN (H1N1) strain (Fig. 2B).

Arbidol blocks authentic LASV infection. To evaluate the efficacy of arbidol against authentic LASV, we performed LASV (Josiah) plaque reduction assays under biosafety level 4 (BSL4) conditions, testing the effects of concentrations of arbidol up to 40 μM. Cells were pretreated with arbidol for 1 h and then infected with LASV (Josiah) in the continued presence of arbidol for 24 h. In the first of three experiments the IC_{50} was ~5 to 10 μM and the maximum inhibition was 98% (Fig. 3A); in the second, the IC_{50} was ~20 μM and the maximum inhibition was 100% (Fig. 3B). In a third experiment, testing only 20 μM arbidol, the percent inhibition was 74% (Fig. 3C). The average percent inhibition caused by 20 μM arbidol from the three experiments was 72.5% (Fig. 3D). By visual inspection 40 μM arbidol had no effect on Vero cell monolayers for up to 5 days (data not shown). We note that the apparent IC_{50} for arbidol versus authentic LASV (Fig. 3) is higher than that seen with MLV pseudoviruses bearing LASV GP (Fig. 1 and 2).

Arbidol blocks LASV GP-mediated fusion. We next asked if arbidol impairs LASV GP-mediated fusion, as it does for other viruses (33, 35, 38, 39, 41). Given that optimal LASV fusion requires the endosomal protein Lamp1 (26, 31, 42), we used cells expressing Lamp1 at the plasma membrane (pmLamp) as fusion targets. Cell-cell fusion (CCF) was then induced between cocultured effector cells (expressing LASV GP at their
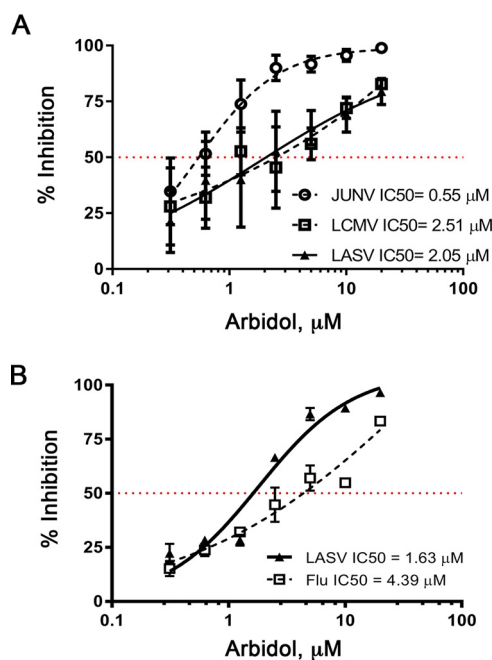
FIG 2 Comparative effects of arbidol on infection by MLV pseudoviruses bearing LASV or other viral glycoproteins: LASV, LCMV, and Junin GP (A) and LASV GP and influenza virus HA (B). MLV pseudoviruses bearing LASV GP, LCMV GP, Junin GP, or WSN influenza HA and NA were prepared as described in Materials and Methods. BSC-1 cells were pretreated with the indicated concentrations of arbidol and then processed and analyzed for infection as described in the legend to Fig. 1. Data in panel A are the averages ± SEMs from three experiments, each performed with triplicate samples. Data in panel B represent the averages ± SDs from triplicate samples from one experiment.

surface) and target cells (expressing Lamp1 at their surface) by briefly exposing the cells to low pH, as described previously (31). To assess the effects of arbidol, effector cells (expressing LASV GP) were pretreated for 1 h with the indicated concentration of arbidol, cocultured with pmLamp1-expressing target cells, and then triggered to fuse by brief exposure to pH 5 (all in the continued presence of arbidol). The efficiency of CCF was then determined by measuring the activity of the luciferase reporter that is functionally restored upon cytoplasmic mixing of fused cells (43). As seen in Fig. 4A, CCF by LASV GP (at pH 5.0) was suppressed by 20 μM and 40 μM arbidol. Based on findings in parallel experiments (Fig. 4B), arbidol appeared more potent at impeding LASV-GP than influenza virus HA-mediated CCF, consistent with its somewhat stronger effect on LASV GP- compared to influenza virus HA-MLV pseudovirus infection (Fig. 2B).

As a complement to the CCF study (Fig. 4), we employed an assay involving forced fusion at the plasma membrane (FFPM) and assessed fusion of LASV GP-vesicular stomatitis virus (VSV) pseudoviruses with the surface of cells expressing pmLamp1 (i.e., with Lamp1 at the cell surface), as previously described (31). As seen in Fig. 5A, arbidol suppressed LASV-GP-mediated FFPM, with strong and complete inhibition seen with 20 and 40 μM doses, respectively. The experiment shown in Fig. 4A was conducted with a pulse at pH 5.0. As seen in Fig. 5B, 40 μM arbidol strongly inhibited LASV GP-mediated FFPM at both pH 5.0 and pH 5.5.

Effects of arbidol on LASV GP1 dissociation. In the case of influenza, arbidol stabilizes HA (the fusion protein) such that the pH dependence for its fusion-inducing conformation change is shifted by 0.2 to 0.3 U in the more acidic direction (37, 39). Stabilization of HA is considered part of the mechanism of arbidol against influenza virus (38, 39, 44, 45). Since two independent assays (CCF and FFPM) showed that arbidol impairs the fusion activity of LASV GP, we next asked whether it impairs a conformational change in GP1 required for fusion activation. Upon exposure to low pH, LASV GP undergoes structural rearrangements, one of the earliest being dissociation of GP1, the
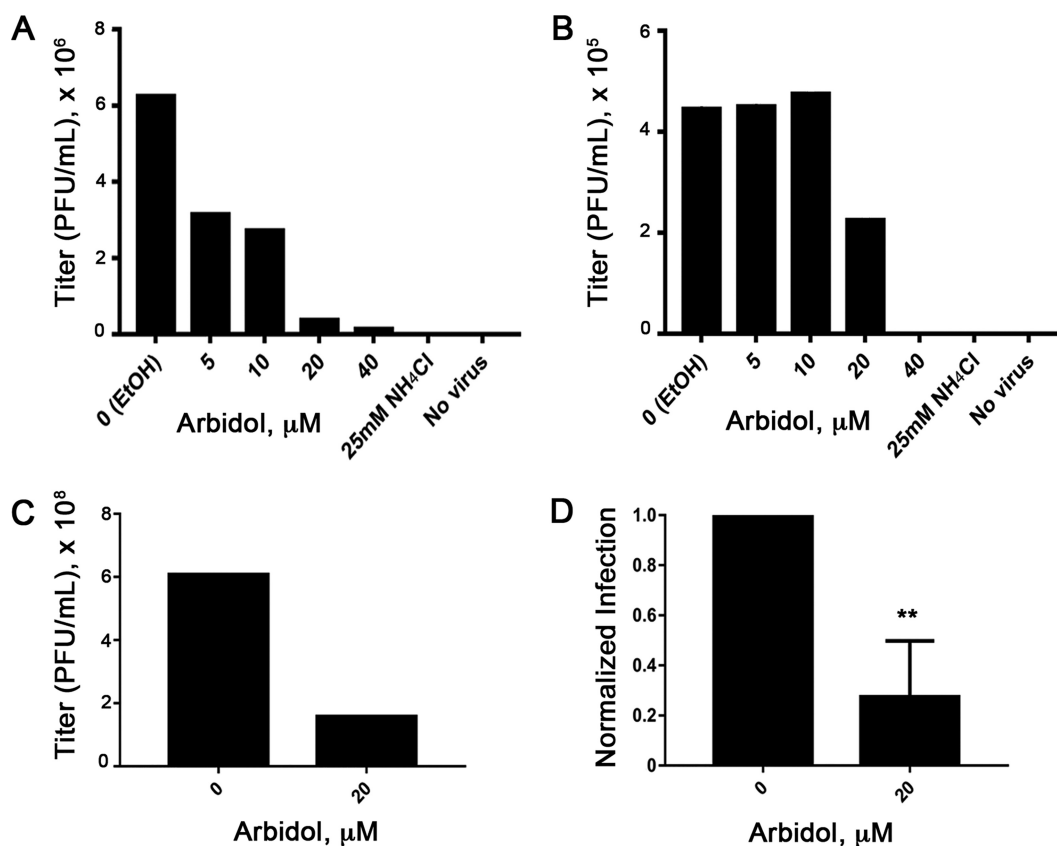
FIG 3 Arbidol inhibits authentic LASV infection. Duplicate wells of Vero 76 cells were pretreated with the indicated concentration of arbidol (or vehicle or 25 mM NH$_4$Cl) for 1 h and then infected with LASV (Josiah strain) virus at an MOI of 0.01. Following a 1-h binding period at 4°C, unadsorbed virus was removed and the cells were incubated for 24 h in the presence of drug in a 37°C CO$_2$ incubator. Culture supernatants were harvested and serially diluted 10-fold in fresh medium, and then titers were determined on Vero 76 cells by a 96-h plaque assay. Results in panels A to C are the average titers from duplicate wells. The values in panel D indicate the average normalized infection in samples treated with 20 μM arbidol ($\pm$SD) from the experiments shown in panels A to C. **, $P < 0.01$.

receptor binding subunit, from GP2, the fusion subunit. This early change is thought to license subsequent changes that allow the fusion loop (in GP2) to access the target membrane and then to permit GP2 to fold back into a trimer of hairpins, which brings the viral and endosomal membranes into intimate contact leading to their fusion (46–49). Experiments using isolated LASV GP1/GP2 captured on beads showed that in this system, dissociation of the 44-kDa GP1 subunit occurs optimally at 37°C and half maximally at pH ~6.4 at 37°C following a 1-min low-pH pulse (data not shown). We therefore treated LASV GP1/GP2 immobilized on beads with either 0 or 40 μM arbidol and then exposed the beads to buffers of different pH values for 1 min at 37°C. As seen in Fig. 6A, the presence of 40 μM arbidol shifted the pH dependence for GP1 dissociation by ~0.5 U in the more acidic direction, suggesting that, as for influenza HA, arbidol can stabilize LASV GP. If arbidol stabilizes LASV GP, then it might delay GP1 dissociation in this system. To test this idea, we again captured LASV GP1/GP2 on beads, pretreated the samples with 0 or 40 μM arbidol, treated the beads at pH 6.5 and 37°C in the presence of arbidol, and then took samples from 0 to 5 min and assayed them for GP1 dissociation. As seen in Fig. 6B, arbidol appeared to introduce an ~30-s lag, thereby slowing GP1 dissociation.

DISCUSSION

Drugs that block LASV and EBOV GP-mediated entry with similar potencies. We began this study by comparing the ability of eight drugs to inhibit LASV and EBOV GP-mediated infection. All eight are orally available, room temperature-stable small
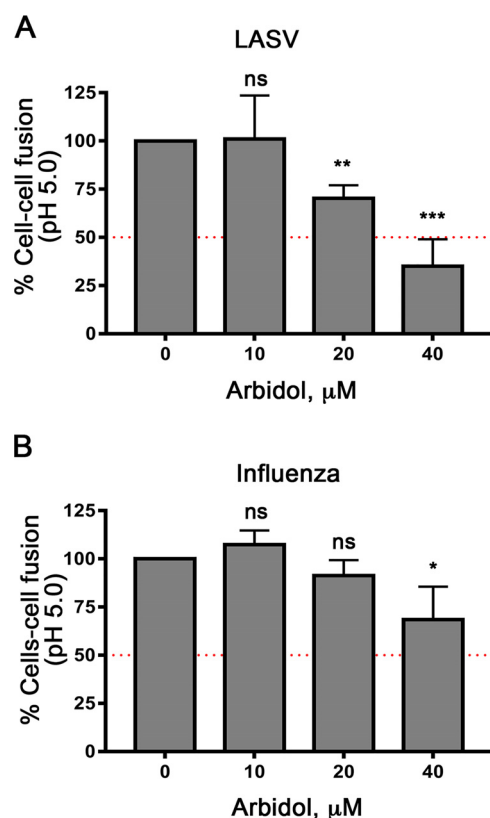
FIG 4 Arbidol suppresses LASV GP-mediated cell-cell fusion (CCF). Effector cells were generated by transfecting HEK293T/17 cells with plasmids encoding DSP_{1-7} (the N-terminal split luciferase plasmid) and either LASV GP (A) or WSN influenza HA and NA (B). Target cells were generated by transfecting HEK293T/17 cells with plasmids encoding DSP_{8-11} (the C-terminal split luciferase plasmid) and pmLamp1. For the experiments, effector cells were preloaded with a luciferase substrate and then pretreated for 1 h with the indicated concentration of arbidol or 10% ethyl alcohol (EtOH; mock control). Effector cells were then cocultured with target HEK293T/17 cells (in the continued presence of arbidol or 10% EtOH) for 3 h at 37°C. At this time the cultures were pulsed with pH 5 buffer for 5 min at 37°C, reneutralized, and then returned to the 37°C CO_2 incubator for 1 h, at which time the luminescent signal was measured. The data represent the normalized luminescent signals (relative to that of the mock-treated controls) from three experiments, each performed with triplicate samples. Error bars indicate SDs. *, $P < 0.05$; **, $P < 0.01$; ***, $P < 0.001$.

molecules that block EBOV entry (18–20, 22, 23, 40, 50) and target entry processes also used by LASV (20–23, 51–53). Six are approved for clinical use and two are in advanced clinical testing. These collective features offer practical advantages (e.g., net costs and ease of transport and delivery) compared to novel drugs, many of which are designed in a "one drug-one bug" approach (54).

Five drugs showed similar potencies against LASV and EBOV GP-mediated entry (Table 1). Zoniporide, an inhibitor of the plasma membrane Na^+/H^+ exchanger, blocks infection by the arenavirus LCMV by thwarting macropinocytotic uptake of viral particles (52). As both LASV (30) and EBOV (55, 56) are taken into cells by macropinocytosis, we expected and found zoniporide to have similar activities against both. Two drugs that impair endosome acidification, needed for the entry of both viruses (25, 49)— amodiaquine (an antimalarial) and niclosamide (an anthelminthic)—also showed similar potencies against these two viral GPs in our direct comparative tests. Both have been shown, albeit not in direct comparative studies, to inhibit many pathogens that enter cells by endocytosis (21–23, 57–60). The fourth drug with similar activity against both viruses is apilimod, which inhibits PIKfyve, an enzyme required for late endosome maturation (51, 53, 61) and EBOV entry (27). Apilimod blocks EBOV trafficking to late endosomes (51, 53), which serve as portals for both EBOV and LASV (25, 26, 62–64). The fifth drug with similar potency against LASV GP- and EBOV GP- mediated entry
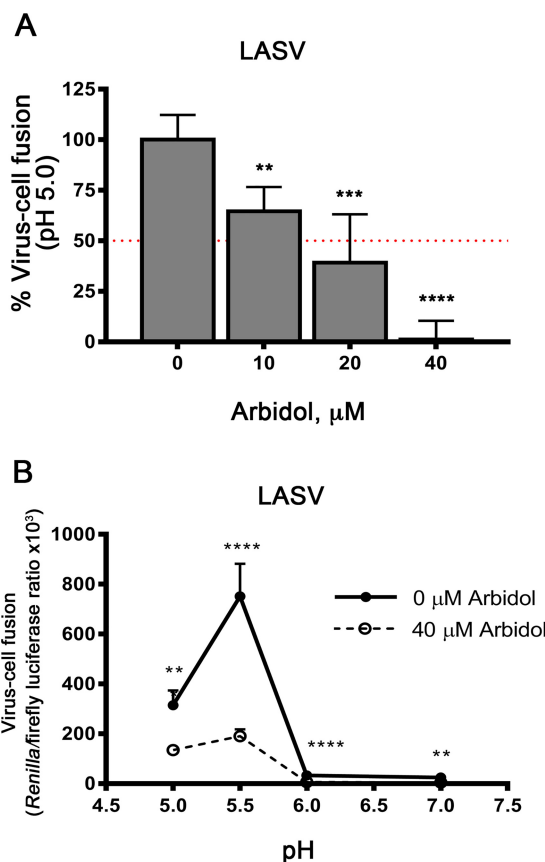
FIG 5 Arbidol inhibits LASV-GP-mediated forced fusion at the plasma membrane (FFPM). COS7 cells were transfected with plasmids encoding pmLamp1 and firefly luciferase (FLUC). Roughly 24 h later, the cells were pretreated with the indicated dose of arbidol (or mock treated) for 1 h. At this time, VSV pseudoviruses bearing LASV GP and encoding *Renilla* luciferase (RLUC) were allowed to bind at 4°C for 1 h. The cells were then pulsed for 5 min at 37°C with prewarmed buffers at either pH 5 (A) or the indicated pH (B), and then the buffer was replaced with complete medium containing NH_4Cl to prevent infection via the normal endocytic route. After 12 to 18 h at 37°C, RLUC (an indicator of infection via FFPM) and FLUC (to standardize transfected cell numbers) were measured. The ratio of *Renilla* to firefly luciferase (RLUC/FLUC) was then normalized to RLUC/FLUC ratio for the mock-treated cells (A) or directly plotted (B). Data are from a representative experiment performed with quintuplicate samples. Error bars indicate SD. ***, $P < 0.001$; ****, $P < 0.0001$. Each experiment was repeated one time, with similar results.

is arbidol (Umifenovir), a synthetic antiviral approved and used in Russia and China to combat influenza and shown to have broad-spectrum antiviral activity (33, 34, 36, 38, 39).

The other three drugs—clomiphene, toremifene, and sertraline—showed ~3- to 6-fold greater activity against EBOV GP- than LASV GP-mediated entry. They are CADs that block EBOV infections (19, 20, 22, 23, 40) and cause cholesterol accumulation in late endosomes, mimicking effects of dysfunctional NPC1, the EBOV receptor (27, 28, 65). Since LASV also enters cells through late endosomes (31), CADs may interfere with LASV entry due to general impairments of late endosome function. The enhanced activity of toremifene and sertraline against EBOV (Table 1) may be because they can bind to both EBOV GP, as shown by thermal stability assays and X-ray crystallography (66, 67), and the viral and/or endosomal membrane (35, 39, 45, 66).

Mechanisms by which arbidol may block LASV entry and infection. Arbidol showed roughly equivalent potencies against LASV and EBOV GP-mediated pseudovirus infection (Fig. 1 and Table 1), blocked infection by authentic LASV (Fig. 3), and was somewhat more effective at blocking LASV GP- versus influenza virus HA-mediated fusion and entry (Fig. 2B and Fig. 4B). Three mechanisms have been proposed for the action of arbidol against influenza: direct binding to HA (K_d [dissociation constant],
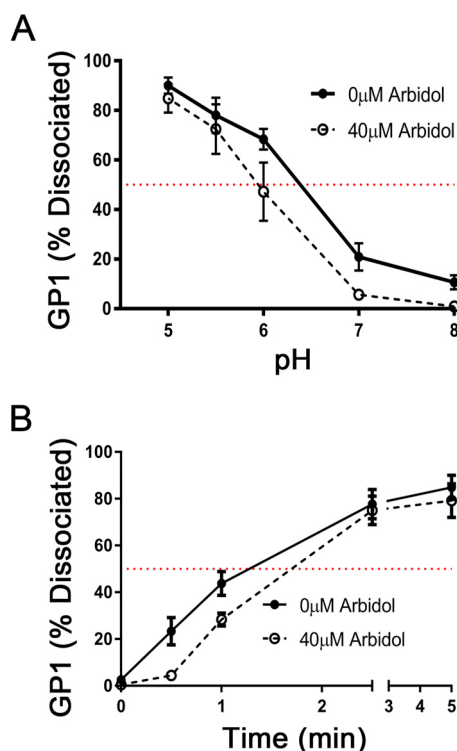
FIG 6 Arbidol impairs LASV GP1 dissociation from GP2. (A) Flag-tagged LASV GP from cell lysates of Lamp1 KO HEK293T/17 cells was immobilized on anti-Flag (M2) magnetic beads, which were then treated with 0 or 40 μM arbidol for 1 h at 4°C. The beads were then subjected to a pulse for 1 min at 37°C at the indicated pH in the presence or absence of arbidol. The extent of GP1 dissociation was then determined by Western blot analysis of GP1 in the supernatant and bead-bound fractions. Data are the averages from four experiments. Error bars represent SEMs. (B) Flag-tagged LASV GP, prepared and immobilized as for panel (A), was pretreated with 0 or 40 μM arbidol. The beads were then exposed to pH 6.5 at 37°C for the indicated time, in the presence or absence of arbidol, and the extent of GP1 dissociation was determined as for panel A. Data are the averages from five experiments. Error bars represent SEMs.

47 μM for binding to PR8 influenza virus HA) (38, 44) and, as proposed for other viruses, binding to the viral and/or target membrane so as to reduce fusion fitness (34, 35). By binding to and stabilizing HA, arbidol shifts the pH threshold for fusion-inducing conformational changes by ~0.2 to 0.3 U in the more acidic direction (37, 38). This is noteworthy, as even such small changes in fusion pH can significantly impact influenza virus infectivity (67). Similarly, we found that arbidol shifts the pH dependence for LASV GP1 dissociation from GP2 by ~0.5 U (in the more acidic direction). This event is thought to unclamp the LASV fusion subunit (GP2), analogous to the unclamping of influenza HA2 and HIV gp41. Hence, in addition to its likely general fusion-impairing effects caused by intercalation into the viral and/or endosomal membrane (35, 45, 66), it is plausible that arbidol additionally affects the stability of LASV GP in a manner similar to its effects on influenza HA (37–39). And, as reviewed elsewhere (36), arbidol may also affect steps upstream or downstream of fusion.

Therapeutic potential of drugs with similar potencies against LASV and EBOV. As reasoned in the introduction, a long-term goal is to identify a drug cocktail that inhibits both LASV and EBOV. Our focus is on orally available, room temperature-stable drugs that target processes used in common for LASV and EBOV entry into cells. In this study, we identified five drugs that target discrete steps of entry and show approximately equal potencies against LASV and EBOV GP-mediated entry: the macropinocytosis inhibitor zoniporide, the endosome acidification inhibitors amodiaquine and niclosamide, the trafficking inhibitor apilimod, and the fusion inhibitor arbidol.

While zoniporide is not approved, it has advanced to phase II clinical trials for treatment of cardiovascular diseases. As an alternate, the FDA-approved drug aripipra-

zole (trade name, Abilify) may have utility. Aripiprazole blocks EBOV infection and synergizes with other entry inhibitors (20, 23). Preliminary data suggest that it blocks EBOV particle internalization as well as LASV GP-mediated infection (laboratory of J. M. White, unpublished data). The endosome acidification inhibitors amodiaquine and niclosamide are orally available and FDA approved to treat malaria and helminthic diseases, respectively. For both, the maximum serum concentration (C_{max}) is within range of the IC_{50} for anti-EBOV/LASV activity (20–23, 57, 68, 69). Newer amodiaquine derivatives (59) or synergistic drug pairs containing amodiaquine or niclosamide and another agent could lower the needed doses (23). And while the trafficking inhibitor apilimod is well tolerated and a potent antagonist of EBOV and LASV (51, 53, 70; also this study), in an early test, it did not protect mice from lethal EBOV challenge (see reference 23), likely due to its inhibition of interleukin 12/23 (IL-12/23) production (reference 61 and K. Rogers, L. Stunz, O. Shtanko, L. Mallinger, J. M. White, M. Schmidt, S. Varga, N. Butler, G. Bishop, and W. Maury, submitted for publication).

Among the fusion inhibitors tested, arbidol emerges as a candidate for future consideration, as it shows similar activities against LASV and EBOV and appears, in our assays, somewhat more potent against LASV- and EBOV GP- versus influenza HA-mediated fusion and entry. Arbidol is approved and used in China and Russia against influenza and has shown strikingly broad antiviral activity (33, 36, 71). A single standard human dose (200 mg) of arbidol yields a C_{max} lower (33, 72–74) than our preliminary indication (Fig. 3) of its IC_{50} against authentic LASV. We note, however, that the estimated IC_{50}s for arbidol against authentic LASV (Fig. 3) and influenza (39, 45, 75) are similar (roughly ~10 μM; variable for different influenza virus strains). As standard dosing of arbidol for influenza is 200 mg three (72) or four (75) times per day, and as arbidol has a long half-life (36), the net (cumulative) C_{max} with multiple daily dosing is expected to be significantly higher (M. Paine, personal communication). Hence, as standard dosing of arbidol is clinically beneficial against influenza (see, for example, reference 75), it may have utility against LASV and EBOV. However, the only modest reduction in titer seen (Fig. 3) coupled with experience with another hemorrhagic fever virus (76) argues against proposing arbidol as a stand-alone therapeutic. A tolerated higher dose of arbidol (74), a new arbidol derivative (39, 44), or a combination of arbidol with another drug (23, 77, 78) might lower the dose needed to be in line with attainable antiviral efficacy. With respect to a potential drug cocktail including arbidol, it is interesting that amantadine, rimantadine, ribavirin, and ribamidil have been reported to enhance the activity of arbidol against influenza (79).

We envision that an orally available, room temperature-stable, approved drug or cocktail of approved drugs could be rapidly deployed for treatment or prophylaxis against (suspected) cases of LASV and EBOV, especially in regions around the globe that are challenged in terms of resources, infrastructure, and accessibility. Such a drug, or drug cocktail, might be valuable before a definitive diagnosis has been made, concurrent with vaccination (e.g., of health care workers and/or first responders to outbreaks), and/or during the setup of ring vaccination. Here we have identified several drugs with these attributes that show similar degrees of inhibition of LASV and EBOV entry. Moreover, three of them—amodiaquine, niclosamide, and arbidol—inhibit multiple enveloped viruses (33, 36, 57, 60, 71, 80–83). Hence, a drug or drug cocktail containing these drugs could inhibit multiple enveloped viruses that enter cells through the endocytic pathway (49).

MATERIALS AND METHODS

Chemicals and cell culture. Dulbecco's modified Eagle's medium (DMEM), phenol-red free DMEM, Opti-MEM (OMEM), sodium pyruvate, antibiotic/antimycotic, trypsin-EDTA (0.05%), phenol-red free trypsin-EDTA (0.5%), and neutral red (NR) were from Thermo Fisher Scientific. Phosphate-buffered saline (PBS) was from Corning. Cosmic Calf serum (CCS), fetal bovine serum (FBS), and supplemented calf serum (SCS) were from HyClone. Fibronectin was from Millipore. Polyethylenimine (PEI) and nonenzymatic cell dissociation solution were from Sigma. Lipofectamine 2000 was from Invitrogen. Toremifene citrate was from Selleck Chemicals. Zoniporide, amodiaquine, niclosamide, and clomiphene citrate were from Sigma. Apilimod was from Axon MedChem. Sertraline hydrochloride was from Toronto Research Chemicals.

Arbidol was synthesized commercially, and the purity and structure of the product were confirmed as described previously (34).

HEK293T/17 and BSC-1 cells were from the ATCC. Lamp1 KO HEK293T/17 cells (clone 1D4) were described by Hulseberg et al. (31). COS7 cells were from the ATCC and a kind gift from Douglas DeSimone at the University of Virginia. BHK-21 cells were from the ATCC and a kind gift from James Casanova at the University of Virginia. Vero 76 cells were from the U.S. Army Medical Research Institute of Infectious Diseases (USAMRIID). HEK293T/17 and BSC-1 cells were maintained in DMEM containing 10% CCS. BHK21 cells were maintained in DMEM containing 10% SCS. COS7 and Lamp1 KO HEK293T/17 cells were maintained in DMEM containing 10% FBS, 1% sodium pyruvate, and 1% antibiotic/antimycotic. Vero 76 cells were maintained in Corning DMEM with 10% Gibco FBS, 1% penicillin-streptomycin, 1% L-glutamine, and 1% sodium pyruvate.

Plasmids and virus. The pCMV-LASV-GPC Josiah strain plasmid was from F. L. Cosset (Université de Lyon, France) via Gregory Melikian (Emory University); the LASV-GPC-Flag pCC421 Josiah strain was from Jason Botten (University of Vermont). VSV-G plasmid was from Michael Whitt (University of Tennessee); pDisplay-EBOV-GPΔ Mayinga strain was from Erica Saphire (Scripps Research Institute). pTG-Luc plasmid was from Jean Dubuisson (Centre National de la Recherche Scientifique, Lille, France) via Gary Whittaker (Cornell University), and pCMV-Gag-Pol plasmid was from Jean Millet and Gary Whittaker (Cornell University) and Jean Dubuisson. Gag-βlaM plasmid was made by James Simmons (University of Virginia). The pcDNA3-luciferase (firefly) plasmid was from Addgene. The DSP$_{1-7}$ and DSP$_{8-11}$ plasmids were from Naoyuki Kondo (Kansai Medical University, Japan). The WSN HA and neuraminidase (NA) plasmids were from Gary Whittaker (Cornell University). Plasmids encoding LCMV GP and Junin virus GP were from Jack Nunberg (University of Montana).

The stock of LASV (Josiah strain) used was generated by infecting Vero E6 cells in complete Eagle's minimal essential medium (EMEM; VWR) containing 10% FBS (HyClone) and 2% L-glutamine (Thermo Fisher Scientific). Infected cells were incubated at 37°C and 5% CO_2. Virus-containing cell culture supernatant was harvested 3 days postinoculation, clarified at 10,000 × g and 4°C for 10 min, and frozen at −80°C. All work with native LASV was conducted in a BSL4 containment suite with personnel in positive-pressure encapsulating suits following appropriate institutional standard operating procedures.

Antibodies and immunoprecipitation reagents. For Western blotting, the mouse anti-LASV-GP L52-134-23A was from USAMRIID and anti-mouse IR680RD was from Licor. For LASV GP bead capture, anti-Flag M2 magnetic beads were from Sigma.

Pseudovirus production. To produce VSV pseudoviruses, 1 × 10^6 BHK-21 cells were seeded in each of multiple 10-cm² dishes. Cells in each dish were transfected with 12 μg of plasmid encoding LASV-GPC using PEI. The following day, cells were infected with 40 μl (per dish) of VSV-ΔG helper virus (from plaque eluates of known titer) encoding *Renilla* luciferase (diluted in serum-free media) for 1 h at 37°C. After infection, cells were washed extensively with cold PBS and incubated overnight in complete DMEM. Supernatants containing pseudoviruses were collected, clarified, and pelleted through a 20% sucrose-HM (20 mM HEPES, 20 mM morpholineethanesulfonic acid [MES], 130 mM NaCl [pH 7.4]) cushion. The pellet was resuspended in 10% sucrose-HM. VSV-ΔG helper virus was produced following the same procedure, by infecting VSV-G transfected cells with eluate from VSV-ΔG plaques.

For MLV pseudoviruses, HEK293T/17 cells were seeded in 10-cm² dishes. The following day, cells were transfected with 6 μg of total DNA using a 2:1:1:1 ratio of pTG-Luc:pCMV Gag-Pol:Gag-βlam:glycoprotein. At 48 h posttransfection, virus-containing medium was harvested, clarified, pelleted through a 20% sucrose-HM cushion, resuspended in 10% sucrose-HM, and stored at −80°C in single-use aliquots.

LASV plaque reduction assay. Vero 76 cells were seeded on 6-well plates. At full confluence, cells in duplicate wells were pretreated with the indicated concentration of arbidol, 25 mM NH$_4$Cl, or 10% ethanol vehicle for 1 h at 37°C. Cells were then infected with LASV at a multiplicity of infection (MOI) of 0.01 for 1 h in the presence of the indicated concentration of arbidol or vehicle. Cells were washed twice to remove unbound virus and incubated for 24 h at 37°C in drug-containing medium. Supernatants were harvested and 10-fold serial dilutions were made to infect ∼90% confluent monolayers of Vero 76 cells in 6-well plates for 1 h at 37°C, with rocking every 15 min. A primary overlay consisting of a 1:1 mixture of 1.6% SeaKem agarose (Lonza) and 2× Eagle's basal medium (Thermo Fisher Scientific) supplemented with 20% FBS and 8% Glutamax (Thermo Fisher Scientific) was then added on top of the infected cells and allowed to solidify. Cells were incubated for 4 days at 37°C, followed by addition of a secondary overlay consisting of a 1:1 mixture identical to the above but with the addition of 8% NR (final concentration was 4%). Plaques were counted the following day. Plaque counts were averaged from duplicate wells and then multiplied by the dilution factor to establish the starting titer of input supernatants.

Biosafety. All manipulations involving live LASV were performed in a biosafety level 4 containment suite at USAMRIID with personnel wearing positive-pressure protective suits fitted with HEPA filters and umbilical-fed air. USAMRIID is registered with the Centers for Disease Control Select Agent Program for the possession and use of biological select agents and toxins and has implemented a biological surety program in accordance with U.S. Army regulation AR 50-1, "Biological Surety."

Pseudovirus infection assay. BSC-1 cells were seeded on white 96-well plates (1.5 × 10^4 cells/well). The following day, cells were pretreated with drugs (or mock) for 1 h in OMEM and then, while maintaining the presence of drug, were infected with an input of EBOV GP- and LASV GP-pseudoviruses adjusted to achieve roughly equivalent RLU signals in the mock-treated samples. After 24 h at 37°C and 5% CO_2, the cells were lysed with Britelite reagent (PerkinElmer) and luminescence was measured. IC$_{50}$s were determined and statistical analysis of all data was performed using GraphPad Prism 7 (GraphPad Software, Inc.): log(agonist) versus response-variable slope (four parameters) constrained to bottom = 0.

Cell-cell fusion (CCF) assay. Effector (HEK293T/17) cells were seeded on 6-well plates (6.75×10^5 cells/well). Target (HEK293T/17) cells were seeded on fibronectin-coated opaque white 96-well plates (3.5×10^4 cells/well). Effector cells were transfected with 1 μg/well of GP plasmid and 1 μg/well of DSP_{1-7} plasmid. Target cells were cotransfected with 33 ng/well of pmLamp1 and 33 ng/well of DSP_{8-11} plasmid. Cells were transfected using Lipofectamine 2000 according to the manufacturer's instructions. Twenty-four hours posttransfection, effector cells were loaded with EnduRen luciferase substrate (Promega) (60 μM in complete DMEM) for 2 h at 37°C. Effector cells were then rinsed with PBS and lifted with nonenzymatic cell dissociation solution. Effector cells were resuspended in complete DMEM and 1×10^5 effector cells were overlaid onto each well of target cells (96-well plate). Cells were cocultured for 3 h. At this time, a low pH pulse was applied with fusion buffer (100 mM NaCl, 15 mM HEPES, 15 mM succinate, 15 mM MES, 2 mg/ml of glucose) adjusted to pH 5.0 for 5 min at 37°C. The pH was reneutralized by replacing the fusion buffer with complete DMEM, and the cells were returned to 37°C for 1 h before measuring luciferase activity.

Forced fusion at the plasma membrane (FFPM) assay. COS7 cells were seeded in 6-well plates (4×10^5 cells/well). Approximately 24 h postseeding, the cells were transfected with 1 μg of plasmid encoding firefly luciferase using Lipofectamine 2000 according to the manufacturer's instructions. Approximately 24 h posttransfection, the cells were washed, lifted, and reseeded at 1.5×10^4 cells/well on fibronectin-coated opaque white 96-well plates. The day after reseeding, cells were chilled on ice for 15 min and LASV-GP VSV-luciferase (*Renilla*) pseudoviruses, an amount determined to reach a target signal of at least 1×10^6 RLUs in a standard infection assay, were added to cells in quintuplicate in serum-free DMEM. Pseudoviruses were bound to the cells by centrifugation ($250 \times g$, 1 h, and 4°C). Cells were returned to ice and washed once with cold PBS. Fusion was triggered by applying a pulse of prewarmed low pH fusion buffer (as in CCF assay) for 5 min at 37°C adjusted to the indicated pH values. Cells were returned to ice, and the fusion buffer was replaced with complete DMEM containing 40 mM NH_4Cl (to block virus entry via the normal endocytic route). Sixteen hours later, luciferase activity was measured using the Dual-Glo luciferase assay system (Promega) according to the manufacturer's instructions using a Promega GloMax luminometer. The ratio of *Renilla* luciferase activity (an indicator for pseudovirus infection) over firefly luciferase activity (to account for the number of cells) was calculated to assess viral GP-mediated fusion with the plasma membrane.

GP1 dissociation assay. Lamp1 KO HEK293T/17 cells were seeded in 6-well plates (6.25×10^5 cells/well). The following day, cells were transfected with 1 μg of LASV-GPC-Flag using PEI. At 48 h posttransfection, the cells were lysed with NETI buffer (150 mM NaCl, 1 mM EDTA, 50 mM Tris-HCl, 0.5% Igepal) at pH 8. After clearing cell debris (centrifugation for 15 min at 21,000 $\times$ g), the lysate was incubated with anti-Flag M2 magnetic beads (that had been prewashed twice in NETI buffer [pH 8]) for 1 h at 4°C. Arbidol was then added to the bead-plus-lysate mixture as indicated, and the samples were incubated for an additional hour at 4°C. For pH-dependent dissociation experiments, beads with captured LASV GP and pretreated with or without arbidol were then pulled over on a magnetic stand and quickly washed with cold NETI buffer (without arbidol) at the desired pH. The cold NETI buffer was then replaced with prewarmed NETI buffer at the same pH with or without arbidol, as indicated. Samples were incubated at 37°C for 1 min. For time-dependent dissociation experiments, beads with captured LASV GP and pretreated with or without arbidol as described above were quickly washed with cold NETI buffer at pH 6.5. The cold pH 6.5 buffer was then replaced with prewarmed NETI buffer at pH 6.5 with or without arbidol. Samples were then incubated at 37°C for 0.5, 1.0, 2.5, or 5.0 min. The "0 min" samples were treated with prewarmed buffer and then placed immediately on ice after buffer addition. At the end of the incubation period, the samples were immediately placed on the magnetic rack and supernatants collected. Proteins were then eluted from the residual beads using 100 mM glycine (pH 3.5) for 15 min at 25°C with constant vortexing, and the eluted samples were neutralized by the addition of 1 M Tris-HCl (pH 8.5). Supernatant and bead samples were then analyzed by SDS-PAGE and Western blotting, with a primary antibody against LASV GP1. The signal intensity of the GP1 bands in the supernatant and corresponding bead samples was measured using ImageJ. Percent GP1 dissociation was calculated as the signal intensity of the GP1 band in the supernatant divided by the summed signal intensity of the GP1 bands in the supernatant and bead samples.

ACKNOWLEDGMENTS

REFERENCES

1. Hallam HJ, Hallam S, Rodriguez SE, Barrett ADT, Beasley DWC, Chua A, Ksiazek TG, Milligan GN, Sathiyamoorthy V, Reece LM. 2018. Baseline mapping of Lassa fever virology, epidemiology and vaccine research and development. NPJ Vaccines 3:11. https://doi.org/10.1038/s41541-018-0049-5.

2. Siddle KJ, Eromon P, Barnes KG, Mehta S, Oguzie JU, Odia I, Schaffner SF, Winnicki SM, Shah RR, Qu J, Wohl S, Brehio P, Iruolagbe C, Aiyepada J, Uyigue E, Akhilomen P, Okonofua G, Ye S, Kayode T, Ajogbasile F, Uwanibe J, Gaye A, Momoh M, Chak B, Kotliar D, Carter A, Gladden-Young A, Freije CA, Omoregie O, Osiemi B, Muoebonam EB, Airende M,

Enigbe R, Ebo B, Nosamiefan I, Oluniyi P, Nekoui M, Ogbaini-Emovon E, Garry RF, Andersen KG, Park DJ, Yozwiak NL, Akpede G, Ihekweazu C, Tomori O, Okogbenin S, Folarin OA, Okokhere PO, MacInnis BL, Sabeti PC, Happi CT. 2018. Genomic analysis of Lassa virus during an increase in cases in Nigeria in 2018. N Engl J Med 379:1745–1753. https://doi.org/10.1056/NEJMoa1804498.

3. Warner BM, Safronetz D, Stein DR. 2018. Current research for a vaccine against Lassa hemorrhagic fever virus. Drug Des Devel Ther 12:2519–2527. https://doi.org/10.2147/DDDT.S147276.

4. Asogun DA, Adomeh DI, Ehimuan J, Odia I, Hass M, Gabriel M, Olschläger S, Becker-Ziaja B, Folarin O, Phelan E, Ehiane PE, Ifeh VE, Uyigue EA, Oladapo YT, Muoebonam EB, Osunde O, Dongo A, Okokhere PO, Okogbenin SA, Momoh M, Alikah SO, Akhuemokhan OC, Imomeh P, Odike MAC, Gire S, Andersen K, Sabeti PC, Happi CT, Akpede GO, Günther S. 2012. Molecular diagnostics for lassa fever at Irrua specialist teaching hospital, Nigeria: lessons learnt from two years of laboratory operation. PLoS Negl Trop Dis 6:e1839. https://doi.org/10.1371/journal.pntd.0001839.

5. Bausch DG, Hadi CM, Khan SH, Lertora JJL. 2010. Review of the literature and proposed guidelines for the use of oral ribavirin as postexposure prophylaxis for Lassa fever. Clin Infect Dis 51:1435–1441. https://doi.org/10.1086/657315.

6. Welch SR, Guerrero LW, Chakrabarti AK, McMullan LK, Flint M, Bluemling GR, Painter GR, Nichol ST, Spiropoulou CF, Albariño CG. 2016. Lassa and Ebola virus inhibitors identified using minigenome and recombinant virus reporter systems. Antiviral Res 136:9–18. https://doi.org/10.1016/j.antiviral.2016.10.007.

7. Goba A, Khan SH, Fonnie M, Fullah M, Moigboi A, Kovoma A, Sinnah V, Yoko N, Rogers H, Safai S, Momoh M, Koroma V, Kamara FK, Konowu E, Yillah M, French I, Mustapha I, Kanneh F, Foday M, McCarthy H, Kallon T, Kallon M, Naiebu J, Sellu J, Jalloh AA, Gbakie M, Kanneh L, Massaly JLB, Kargbo D, Kargbo B, Vandi M, Gbetuwa M, Gevao SM, Sandi JD, Jalloh SC, Grant DS, Blyden SO, Crozier I, Schieffelin JS, McLellan SL, Jacob ST, Boisen ML, Hartnett JN, Cross RW, Branco LM, Andersen KG, Yozwiak NL, Gire SK, Tariyal R, Park DJ, Haislip AM, Bishop CM, Melnik LI, Gallaher WR, Wimley WC, He J, Shaffer JG, Sullivan BM, Grillo S, Oman S, Garry CE, Edwards DR, McCormick SJ, Elliott DH, Rouelle JA, Kannadka CB, Reyna AA, Bradley BT, Yu H, Yenni RE, Hastie KM, Geisbert JB, Kulakosky PC, Wilson RB, Oldstone MBA, Pitts KR, Henderson LA, Robinson JE, Geisbert TW, Saphire EO, Happi CT, Asogun DA, Sabeti PC, Garry RF, Viral Hemorrhagic Fever Consortium. 2016. An outbreak of Ebola virus disease in the Lassa fever zone. J Infect Dis 214:S110–S121. https://doi.org/10.1093/infdis/jiw239.

8. Wang P, Liu Y, Zhang G, Wang S, Guo J, Cao J, Jia X, Zhang L, Xiao G, Wang W. 2018. Screening and identification of Lassa virus entry inhibitors from an FDA-approved drug library. J Virol 92:e00954-18. https://doi.org/10.1128/JVI.00954-18.

9. Ngo N, Henthorn KS, Cisneros MI, Cubitt B, Iwasaki M, de la Torre JC, Lama J. 2015. Identification and mechanism of action of a novel small-molecule inhibitor of arenavirus multiplication. J Virol 89:10924–10933. https://doi.org/10.1128/JVI.01587-15.

10. Rathbun JY, Droniou ME, Damoiseaux R, Haworth KG, Henley JE, Exline CM, Choe H, Cannon PM. 2015. Novel arenavirus entry inhibitors discovered by using a minigenome rescue system for high-throughput drug screening. J Virol 89:8428–8443. https://doi.org/10.1128/JVI.00997-15.

11. Shankar S, Whitby LR, Casquilho-Gray HE, York J, Boger DL, Nunberg JH. 2016. Small-molecule fusion inhibitors bind the pH-sensing stable signal peptide-GP2 subunit interface of the Lassa virus envelope glycoprotein. J Virol 90:6799–6807. https://doi.org/10.1128/JVI.00597-16.

12. Wang MK-M, Ren T, Liu H, Lim S-Y, Lee K, Honko A, Zhou H, Dyall J, Hensley L, Gartin AK, Cunningham JM. 2018. Critical role for cholesterol in Lassa fever virus entry identified by a novel small molecule inhibitor targeting the viral receptor LAMP1. PLoS Pathog 14:e1007322. https://doi.org/10.1371/journal.ppat.1007322.

13. Burgeson JR, Moore AL, Gharaibeh DN, Larson RA, Cerruti NR, Amberg SM, Hruby DE, Dai D. 2013. Discovery and optimization of potent broad-spectrum arenavirus inhibitors derived from benzimidazole and related heterocycles. Bioorg Med Chem Lett 23:750–756. https://doi.org/10.1016/j.bmcl.2012.11.093.

14. Rosenke K, Feldmann H, Westover JB, Hanley PW, Martellaro C, Feldmann F, Saturday G, Lovaglio J, Scott DP, Furuta Y, Komeno T, Gowen BB, Safronetz D. 2018. Use of favipiravir to treat Lassa virus infection in macaques. Emerg Infect Dis 24:1696–1699. https://doi.org/10.3201/eid2409.180233.

15. Urata S, Yun N, Pasquato A, Paessler S, Kunz S, de la Torre JC. 2011. Antiviral activity of a small-molecule inhibitor of arenavirus glycoprotein processing by the cellular site 1 protease. J Virol 85:795–803. https://doi.org/10.1128/JVI.02019-10.

16. Mohr EL, McMullan LK, Lo MK, Spengler JR, Bergeron É, Albariño CG, Shrivastava-Ranjan P, Chiang C-F, Nichol ST, Spiropoulou CF, Flint M. 2015. Inhibitors of cellular kinases with broad-spectrum antiviral activity for hemorrhagic fever viruses. Antiviral Res 120:40–47. https://doi.org/10.1016/j.antiviral.2015.05.003.

17. Chou Y-Y, Cuevas C, Carocci M, Stubbs SH, Ma M, Cureton DK, Chao L, Evesson F, He K, Yang PL, Whelan SP, Ross SR, Kirchhausen T, Gaudin R. 2016. Identification and characterization of a novel broad-spectrum virus entry inhibitor. J Virol 90:4494–4510. https://doi.org/10.1128/JVI.00103-16.

18. Gehring G, Rohrmann K, Atenchong N, Mittler E, Becker S, Dahlmann F, Pöhlmann S, Vondran FWR, David S, Manns MP, Ciesek S, von Hahn T. 2014. The clinically approved drugs amiodarone, dronedarone and verapamil inhibit filovirus cell entry. J Antimicrob Chemother 69:2123–2131. https://doi.org/10.1093/jac/dku091.

19. Johansen LM, Brannan JM, Delos SE, Shoemaker CJ, Stossel A, Lear C, Hoffstrom BG, DeWald LE, Schornberg KL, Scully C, Lehar J, Hensley LE, White JM, Olinger GG. 2013. FDA-approved selective estrogen receptor modulators inhibit Ebola virus infection. Sci Transl Med 5:190ra79. https://doi.org/10.1126/scitranslmed.3005471.

20. Johansen LM, DeWald LE, Shoemaker CJ, Hoffstrom BG, Lear-Rooney CM, Stossel A, Nelson E, Delos SE, Simmons JA, Grenier JM, Pierce LT, Pajouhesh H, Lehár J, Hensley LE, Glass PJ, White JM, Olinger GG. 2015. A screen of approved drugs and molecular probes identifies therapeutics with anti-Ebola virus activity. Sci Transl Med 7:290ra89. https://doi.org/10.1126/scitranslmed.aaa5597.

21. Madrid PB, Chopra S, Manger ID, Gilfillan L, Keepers TR, Shurtleff AC, Green CE, Iyer LV, Dilks HH, Davey RA, Kolokoltsov AA, Carrion R, Patterson JL, Bavari S, Panchal RG, Warren TK, Wells JB, Moos WH, Burke RL, Tanga MJ. 2013. A systematic screen of FDA-approved drugs for inhibitors of biological threat agents. PLoS One 8:e60579. https://doi.org/10.1371/journal.pone.0060579.

22. Kouznetsova J, Sun W, Martínez-Romero C, Tawa G, Shinn P, Chen CZ, Schimmer A, Sanderson P, McKew JC, Zheng W, García-Sastre A. 2014. Identification of 53 compounds that block Ebola virus-like particle entry via a repurposing screen of approved drugs. Emerg Microbes Infect 3:e84. https://doi.org/10.1038/emi.2014.88.

23. Dyall J, Nelson EA, DeWald LE, Guha R, Hart BJ, Zhou H, Postnikova E, Logue J, Vargas WM, Gross R, Michelotti J, Deiuliis N, Bennett RS, Crozier I, Holbrook MR, Morris PJ, Klumpp-Thomas C, McKnight C, Mierzwa T, Shinn P, Glass PJ, Johansen LM, Jahrling PB, Hensley LE, Olinger GG, Jr, Thomas C, White JM. 2018. Identification of combinations of approved drugs with synergistic activity against Ebola virus in cell cultures. J Infect Dis 218:S672–S678. https://doi.org/10.1093/infdis/jiy304.

24. Rhein BA, Maury WJ. 2015. Ebola virus entry into host cells: identifying therapeutic strategies. Curr Clin Microbiol Rep 2:115–124. https://doi.org/10.1007/s40588-015-0021-3.

25. Jae LT, Brummelkamp TR. 2015. Emerging intracellular receptors for hemorrhagic fever viruses. Trends Microbiol 23:1–9.

26. Jae LT, Raaben M, Herbert AS, Kuehne AI, Wirchnianski AS, Soh TK, Stubbs SH, Janssen H, Damme M, Saftig P, Whelan SP, Dye JM, Brummelkamp TR. 2014. Lassa virus entry requires a trigger-induced receptor switch. Science 344:1506–1510. https://doi.org/10.1126/science.1252480.

27. Carette JE, Raaben M, Wong AC, Herbert AS, Obernosterer G, Mulherkar N, Kuehne AI, Kranzusch PJ, Griffin AM, Ruthel G, Cin PD, Dye JM, Whelan SP, Chandran K, Brummelkamp TR. 2011. Ebola virus entry requires the cholesterol transporter Niemann-Pick C1. Nature 477:340–343. https://doi.org/10.1038/nature10348.

28. Côté M, Misasi J, Ren T, Bruchez A, Lee K, Filone CM, Hensley L, Li Q, Ory D, Chandran K, Cunningham J. 2011. Small molecule inhibitors reveal Niemann-Pick C1 is essential for Ebola virus infection. Nature 477:344–348. https://doi.org/10.1038/nature10380.

29. Brouillette RB, Phillips EK, Patel R, Mahaud-Fernandez W, Moller-Tank S, Rogers KJ, Dillard JA, Cooney AL, Martinez-Sobrido L, Okeoma C, Maury W. 2018. TIM-1 mediates dystroglycan-independent entry of Lassa virus. J Virol 92:e00093-18. https://doi.org/10.1128/JVI.00093-18.

30. Oppliger J, Torriani G, Herrador A, Kunz S. 2016. Lassa virus cell entry via dystroglycan involves an unusual pathway of macropinocytosis. J Virol 90:6412–6429. https://doi.org/10.1128/JVI.00257-16.

31. Hulseberg CE, Fénéant L, Szymańska KM, White JM. 2018. Lamp1 in-

creases the efficiency of Lassa virus infection by promoting fusion in less acidic endosomal compartments. mBio 9:e01818-17. https://doi.org/10.1128/mBio.01818-17.

32. Fedeli C, Moreno H, Kunz S. 2018. Novel insights into cell entry of emerging human pathogenic arenaviruses. J Mol Biol 430:1839–1852. https://doi.org/10.1016/j.jmb.2018.04.026.

33. Fink SL, Vojtech L, Wagoner J, Slivinski NSJ, Jackson KJ, Wang R, Khadka S, Luthra P, Basler CF, Polyak SJ. 2018. The antiviral drug arbidol inhibits Zika virus. Sci Rep 8:8989. https://doi.org/10.1038/s41598-018-27224-4.

34. Pécheur E-I, Borisevich V, Halfmann P, Morrey JD, Smee DF, Prichard M, Mire CE, Kawaoka Y, Geisbert TW, Polyak SJ. 2016. The synthetic antiviral drug arbidol inhibits globally prevalent pathogenic viruses. J Virol 90:3086–3092. https://doi.org/10.1128/JVI.02077-15.

35. Teissier E, Zandomeneghi G, Loquet A, Lavillette D, Lavergne J-P, Montserret R, Cosset F-L, Böckmann A, Meier BH, Penin F, Pécheur E-I. 2011. Mechanism of inhibition of enveloped virus membrane fusion by the antiviral drug arbidol. PLoS One 6:e15874. https://doi.org/10.1371/journal.pone.0015874.

36. Blaising J, Polyak SJ, Pécheur E-I. 2014. Arbidol as a broad-spectrum antiviral: an update. Antiviral Res 107:84–94. https://doi.org/10.1016/j.antiviral.2014.04.006.

37. Leneva IA, Russell RJ, Boriskin YS, Hay AJ. 2009. Characteristics of arbidol-resistant mutants of influenza virus: implications for the mechanism of anti-influenza action of arbidol. Antiviral Res 81:132–140. https://doi.org/10.1016/j.antiviral.2008.10.009.

38. Kadam RU, Wilson IA. 2017. Structural basis of influenza virus fusion inhibition by the antiviral drug arbidol. Proc Natl Acad Sci U S A 114:206–214. https://doi.org/10.1073/pnas.1617020114.

39. Brancato V, Peduto A, Wharton S, Martin S, More V, Di Mola A, Massa A, Perfetto B, Donnarumma G, Schiraldi C, Tufano MA, de Rosa M, Filosa R, Hay A. 2013. Design of inhibitors of influenza virus membrane fusion: synthesis, structure-activity relationship and in vitro antiviral activity of a novel indole series. Antiviral Res 99:125–135. https://doi.org/10.1016/j.antiviral.2013.05.005.

40. Shoemaker CJ, Schornberg KL, Delos SE, Scully C, Pajouhesh H, Olinger GG, Johansen LM, White JM. 2013. Multiple cationic amphiphiles induce a Niemann-Pick C phenotype and inhibit Ebola virus entry and infection. PLoS One 8:e56265. https://doi.org/10.1371/journal.pone.0056265.

41. Boriskin YS, Pécheur E-I, Polyak SJ. 2006. Arbidol: a broad-spectrum antiviral that inhibits acute and chronic HCV infection. Virol J 3:56. https://doi.org/10.1186/1743-422X-3-56.

42. Cohen-Dvashi H, Israeli H, Shani O, Katz A, Diskin R. 2016. Role of LAMP1 binding and pH sensing by the spike complex of Lassa virus. J Virol 90:10329–10338. https://doi.org/10.1128/JVI.01624-16.

43. Kondo N, Miyauchi K, Matsuda Z. 2011. Monitoring viral-mediated membrane fusion using fluorescent reporter methods. Curr Protoc Cell Biol Chapter 26:Unit 26.9. https://doi.org/10.1002/0471143030.cb2609s50.

44. Wright ZVF, Wu NC, Kadam RU, Wilson IA, Wolan DW. 2017. Structure-based optimization and synthesis of antiviral drug Arbidol analogues with significantly improved affinity to influenza hemagglutinin. Bioorg Med Chem Lett 27:3744–3748. https://doi.org/10.1016/j.bmcl.2017.06.074.

45. Boriskin YS, Leneva IA, Pecheur EI, Polyak SP. 2008. Arbidol: a broad-spectrum antiviral compound that blocks viral fusion. Curr Med Chem 15:997–1005. https://doi.org/10.2174/092986708784049658.

46. Illick MM, Branco LM, Fair JN, Illick KA, Matschiner A, Schoepp R, Garry RF, Guttieri MC. 2008. Uncoupling GP1 and GP2 expression in the Lassa virus glycoprotein complex: implications for GP1 ectodomain shedding. Virol J 5:161. https://doi.org/10.1186/1743-422X-5-161.

47. Klewitz C, Klenk H-D, ter Meulen J. 2007. Amino acids from both N-terminal hydrophobic regions of the Lassa virus envelope glycoprotein GP-2 are critical for pH-dependent membrane fusion and infectivity. J Gen Virol 88:2320–2328. https://doi.org/10.1099/vir.0.82950-0.

48. Li S, Sun Z, Pryce R, Parsy M-L, Fehling SK, Schlie K, Siebert CA, Garten W, Bowden TA, Strecker T, Huiskonen JT. 2016. Acidic pH-induced conformations and LAMP1 binding of the Lassa virus glycoprotein spike. PLoS Pathog 12:e1005418. https://doi.org/10.1371/journal.ppat.1005418.

49. White JM, Whittaker GR. 2016. Fusion of enveloped viruses in endosomes. Traffic 17:593–614. https://doi.org/10.1111/tra.12389.

50. Madrid PB, Panchal RG, Warren TK, Shurtleff AC, Endsley AN, Green CE, Kolokoltsov A, Davey R, Manger ID, Gilfillan L, Bavari S, Tanga MJ. 2015. Evaluation of Ebola virus inhibitors for drug repurposing. ACS Infect Dis 1:317–326. https://doi.org/10.1021/acsinfecdis.5b00030.

51. Nelson EA, Dyall J, Hoenen T, Barnes AB, Zhou H, Liang JY, Michelotti J,

Dewey WH, DeWald LE, Bennett RS, Morris PJ, Guha R, Klumpp-Thomas C, McKnight C, Chen Y-C, Xu X, Wang A, Hughes E, Martin S, Thomas C, Jahrling PB, Hensley LE, Olinger GG, White JM. 2017. The phosphatidylinositol-3-phosphate 5-kinase inhibitor apilimod blocks filoviral entry and infection. PLoS Negl Trop Dis 11:e0005540. https://doi.org/10.1371/journal.pntd.0005540.

52. Iwasaki M, Ngo N, de la Torre JC. 2014. Sodium hydrogen exchangers contribute to arenavirus cell entry. J Virol 88:643–654. https://doi.org/10.1128/JVI.02110-13.

53. Qiu S, Leung A, Bo Y, Kozak RA, Anand SP, Warkentin C, Salambanga FDR, Cui J, Kobinger G, Kobasa D, Côté M. 2018. Ebola virus requires phosphatidylinositol (3,5) bisphosphate production for efficient viral entry. Virology 513:17–28. https://doi.org/10.1016/j.virol.2017.09.028.

54. Vigant F, Santos NC, Lee B. 2015. Broad-spectrum antivirals against viral fusion. Nat Rev Microbiol 13:426–437. https://doi.org/10.1038/nrmicro3475.

55. Saeed MF, Kolokoltsov AA, Albrecht T, Davey RA. 2010. Cellular entry of Ebola virus involves uptake by a macropinocytosis-like mechanism and subsequent trafficking through early and late endosomes. PLoS Pathog 6:e1001110. https://doi.org/10.1371/journal.ppat.1001110.

56. Nanbo A, Imai M, Watanabe S, Noda T, Takahashi K, Neumann G, Halfmann P, Kawaoka Y. 2010. Ebolavirus is internalized into host cells via macropinocytosis in a viral glycoprotein-dependent manner. PLoS Pathog 6:e1001121. https://doi.org/10.1371/journal.ppat.1001121.

57. Jurgeit A, McDowell R, Moese S, Meldrum E, Schwendener R, Greber UF. 2012. Niclosamide is a proton carrier and targets acidic endosomes with broad antiviral effects. PLoS Pathog 8:e1002976. https://doi.org/10.1371/journal.ppat.1002976.

58. Zilbermintz L, Leonardi W, Jeong S-Y, Sjodt M, McComb R, Ho C-LC, Retterer C, Gharaibeh D, Zamani R, Soloveva V, Bavari S, Levitin A, West J, Bradley KA, Clubb RT, Cohen SN, Gupta V, Martchenko M. 2015. Identification of agents effective against multiple toxins and viruses by host-oriented cell targeting. Sci Rep 5:13476. https://doi.org/10.1038/srep13476.

59. Sakurai Y, Sakakibara N, Toyama M, Baba M, Davey RA. 2018. Novel amodiaquine derivatives potently inhibit Ebola virus infection. Antiviral Res 160:175–182. https://doi.org/10.1016/j.antiviral.2018.10.025.

60. Marois I, Cloutier A, Meunier I, Weingartl HM, Cantin AM, Richter MV. 2014. Inhibition of influenza virus replication by targeting broad host cell pathways. PLoS One 9:e110631. https://doi.org/10.1371/journal.pone.0110631.

61. Cai X, Xu Y, Cheung AK, Tomlinson RC, Alcázar-Román A, Murphy L, Billich A, Zhang B, Feng Y, Klumpp M, Rondeau J-M, Fazal AN, Wilson CJ, Myer V, Joberty G, Bouwmeester T, Labow MA, Finan PM, Porter JA, Ploegh HL, Baird D, De Camilli P, Tallarico JA, Huang Q. 2013. PIKfyve, a class III PI kinase, is the target of the small molecular IL-12/IL-23 inhibitor apilimod and a player in Toll-like receptor signaling. Chem Biol 20:912–921. https://doi.org/10.1016/j.chembiol.2013.05.010.

62. Mingo RM, Simmons JA, Shoemaker CJ, Nelson EA, Schornberg KL, D'Souza RS, Casanova JE, White JM. 2015. Ebola virus and severe acute respiratory syndrome coronavirus display late cell entry kinetics: evidence that transport to NPC1+ endolysosomes is a rate-defining step. J Virol 89:2931–2943. https://doi.org/10.1128/JVI.03398-14.

63. Simmons JA, D'Souza RS, Ruas M, Galione A, Casanova JE, White JM. 2016. Ebolavirus glycoprotein directs fusion through NPC1+ endolysosomes. J Virol 90:605–610. https://doi.org/10.1128/JVI.01828-15.

64. Spence JS, Krause TB, Mittler E, Jangra RK, Chandran K. 2016. Direct visualization of Ebola virus fusion triggering in the endocytic pathway. mBio 7:e01857-15. https://doi.org/10.1128/mBio.01857-15.

65. Miller EH, Obernosterer G, Raaben M, Herbert AS, Deffieu MS, Krishnan A, Ndungo E, Sandesara RG, Carette JE, Kuehne AI, Ruthel G, Pfeffer SR, Dye JM, Whelan SP, Brummelkamp TR, Chandran K. 2016. Ebola virus entry requires the host-programmed recognition of an intracellular receptor. EMBO J 31:1–14.

66. Pécheur E-I, Lavillette D, Alcaras F, Molle J, Boriskin YS, Roberts M, Cosset F-L, Polyak SJ. 2007. Biochemical mechanism of hepatitis C virus inhibition by the broad-spectrum antiviral arbidol. Biochemistry 46:6050–6059. https://doi.org/10.1021/bi700181j.

67. Gerlach T, Hensen L, Matrosovich T, Bergmann J, Winkler M, Peteranderl C, Klenk H-D, Weber F, Herold S, Pöhlmann S, Matrosovich M. 2017. pH optimum of hemagglutinin-mediated membrane fusion determines sensitivity of influenza A viruses to the interferon-induced antiviral state and IFITMs. J Virol 91:e00246-17. https://doi.org/10.1128/JVI.00246-17.

68. Andrews P, Thyssen J, Lorke D. 1982. The biology and toxicology of

molluscicides, Bayluscide (p282). Pharmacol Ther 19:245–295. https://doi
.org/10.1016/0163-7258(82)90064-X.

69. Bixler SL, Duplantier AJ, Bavari S. 2017. Discovering drugs for the treat-
ment of Ebola virus. Curr Treat Options Infect Dis 9:299–317. https://doi
.org/10.1007/s40506-017-0130-z.

70. Krausz S, Boumans MJH, Gerlag DM, Lufkin J, van Kuijk AWR, Bakker A,
de Boer M, Lodde BM, Reedquist KA, Jacobson EW, O'Meara M, Tak PP.
2012. Brief report: a phase IIa, randomized, double-blind, placebo-
controlled trial of apilimod mesylate, an interleukin-12/interleukin-23
inhibitor, in patients with rheumatoid arthritis. Arthritis Rheum 64:
1750–1755. https://doi.org/10.1002/art.34339.

71. Haviernik J, Štefánik M, Fojtíková M, Kali S, Tordo N, Rudolf I, Hubálek Z,
Eyer L, Ruzek D. 2018. Arbidol (umifenovir): a broad-spectrum antiviral
drug that inhibits medically important arthropod-borne flaviviruses.
Viruses 10:E184. https://doi.org/10.3390/v10040184.

72. Deng P, Zhong D, Yu K, Zhang Y, Wang T, Chen X. 2013. Pharmacoki-
netics, metabolism, and excretion of the antiviral drug arbidol in hu-
mans. Antimicrob Agents Chemother 57:1743–1755. https://doi.org/10
.1128/AAC.02282-12.

73. Liu M-Y, Wang S, Yao W-F, Wu H-Z, Meng S-N, Wei M-J. 2009. Pharma-
cokinetic properties and bioequivalence of two formulations of arbidol:
an open-label, single-dose, randomized-sequence, two-period crossover
study in healthy Chinese male volunteers. Clin Ther 31:784–792. https://
doi.org/10.1016/j.clinthera.2009.04.016.

74. Sun Y, He X, Qiu F, Zhu X, Zhao M, Li-Ling J, Su X, Zhao L. 2013.
Pharmacokinetics of single and multiple oral doses of arbidol in healthy
Chinese volunteers. Int J Clin Pharmacol Ther 51:423–432. https://doi
.org/10.5414/CP201843.

75. Leneva IA, Burtseva EI, Yatsyshina SB, Fedyakina IT, Kirillova ES, Selkova
EP, Osipova E, Maleev VV. 2016. Virus susceptibility and clinical effec-
tiveness of anti-influenza drugs during the 2010-2011 influenza season
in Russia. Int J Infect Dis 43:77–84. https://doi.org/10.1016/j.ijid.2016.01
.001.

76. Oestereich L, Rieger T, Neumann M, Bernreuther C, Lehmann M, Krase-
mann S, Wurr S, Emmerich P, de Lamballerie X, Olschläger S, Günther
S. 2014. Evaluation of antiviral efficacy of ribavirin, arbidol, and T-705
(favipiravir) in a mouse model for Crimean-Congo hemorrhagic fever.
PLoS Negl Trop Dis 8:e2804. https://doi.org/10.1371/journal.pntd
.0002804.

77. Oestereich L, Rieger T, Lüdtke A, Ruibal P, Wurr S, Pallasch E, Bockholt S,
Krasemann S, Muñoz-Fontela C, Günther S. 2016. Efficacy of favipiravir
alone and in combination with ribavirin in a lethal, immunocompetent
mouse model of Lassa fever. J Infect Dis 213:934–938. https://doi.org/
10.1093/infdis/jiv522.

78. Westover JB, Sefing EJ, Bailey KW, Van Wettere AJ, Jung K-H, Dagley A,
Wandersee L, Downs B, Smee DF, Furuta Y, Bray M, Gowen BB. 2016.
Low-dose ribavirin potentiates the antiviral activity of favipiravir against
hemorrhagic fever viruses. Antiviral Res 126:62–68. https://doi.org/10
.1016/j.antiviral.2015.12.006.

79. Leneva IA, Fedyakina IT, Guskova TA, Glushkov RG. 2005. Sensitivity of
various influenza virus strains to arbidol. Influence of arbidol in combi-
nation with other antiviral drugs on reproduction of influenza virus A.
Ter Arkh 77:84–88. (In Russian.)

80. Dyall J, Coleman CM, Hart BJ, Venkataraman T, Holbrook MR, Kindrachuk
J, Johnson RF, Olinger GG, Jahrling PB, Laidlaw M, Johansen LM, Lear-
Rooney CM, Glass PJ, Hensley LE, Frieman MB. 2014. Repurposing of
clinically developed drugs for treatment of Middle East respiratory
syndrome coronavirus infection. Antimicrob Agents Chemother 58:
4885–4893. https://doi.org/10.1128/AAC.03036-14.

81. Xu M, Lee EM, Wen Z, Cheng Y, Huang W-K, Qian X, Tcw J, Kouznetsova
J, Ogden SC, Hammack C, Jacob F, Nguyen HN, Itkin M, Hanna C, Shinn
P, Allen C, Michael SG, Simeonov A, Huang W, Christian KM, Goate A,
Brennand KJ, Huang R, Xia M, Ming G-L, Zheng W, Song H, Tang H. 2016.
Identification of small-molecule inhibitors of Zika virus infection and
induced neural cell death via a drug repurposing screen. Nat Med
22:1101–1107. https://doi.org/10.1038/nm.4184.

82. Kao J-C, HuangFu W-C, Tsai T-T, Ho M-R, Jhan M-K, Shen T-J, Tseng P-C,
Wang Y-T, Lin C-F. 2018. The antiparasitic drug niclosamide inhibits
dengue virus infection by interfering with endosomal acidification inde-
pendent of mTOR. PLoS Negl Trop Dis 12:e0006715. https://doi.org/10
.1371/journal.pntd.0006715.

83. Wang Y-M, Lu J-W, Lin C-C, Chin Y-F, Wu T-Y, Lin L-I, Lai Z-Z, Kuo S-C, Ho
Y-J. 2016. Antiviral activities of niclosamide and nitazoxanide against
chikungunya virus entry and transmission. Antiviral Res 135:81–90.
https://doi.org/10.1016/j.antiviral.2016.10.003.